Two Phases Flows Unstructured Grid Solver: Application to Tsunami Wave Impact

Alioune Nar Sambe
Laboratoire de Sondages Electromagnétiques de l'Environnement Terrestre,
et Institut de Mathématiques de Toulon, Université du Sud Toulon Var
La Garde, France

Frédéric Golay
Institut de Mathématiques de Toulon, Université du Sud Toulon Var
La Garde, France

Damien Sous, Philippe Fraunié, Vincent Rey
Laboratoire de Sondages Electromagnétiques de l'Environnement Terrestre, Université du Sud Toulon Var
Centre national de la recherche Scientifique La Garde, France

Richard Marcer, Christine De Jouette
Principia R&D
La Ciotat, France

ABSTRACT

This paper describes CFD of incompressible air-water flows by solving Euler equations with a two phases flow model leading to an hyperbolic system of conservation laws solved with a finite volume discretization on unstructured grids. An artificial compressibility approach allows a fully explicit scheme for an efficient parallel implementation. The numerical model is based on a low Mach number preconditioning and a second order Riemann solver. Applications to breaking waves on a 15% slope with and without influence of macro-roughness are performed concerning impact and run-up processes on the beach.

KEY WORDS: Wave breaking, finite volume, Godunov scheme, air-water interface, run-up, macro-roughness.

INTRODUCTION

Great improvements have been brought to the knowledge of the hydrodynamics and the general processes occurring in the surf zone, widely affected by the breaking waves (Peregrine 1983, Christensen et al. 2006).
Indeed, the breaking waves play a very important role in marine hydrodynamics, both for ocean physics and engineering applications. Breaking is the most dominant phenomenon in surface wave energy budget. In the naval hydrodynamics context, as for coastal dynamics, a reliable and fast model is necessary to perform parametric investigation to optimize sea defence systems. In particular, kinematics of impact and run up on structures and beaches are drastically important in the case of hazardous events like surges and tsunamis.
Concerning wave breaking modelling, the classical full Navier-Stokes solvers are time consuming (e.g. Vincent et al 2004, Guignard et al 2001, Biausser et al 2004) whereas fast models based on Boussinesq equations are unable to compute wave breaking (Grilli et al, 1989, 2001, Guyenne et al. 2006). Herein a new fast three-dimensional two phases flow solver is presented, based on a finite volume discretization on unstructured grids with subdomains decomposition allowing an efficient parallel implementation. This model has already been validated on Yasuda et al (1997) experimental and numerical test case with convincing numerical performances and computational time (Helluy et al, 2005).

Here, we use a two phase flows model where equations of conservation are solved in a single domain by introducing a state equation depending on the volume fraction of water and air (Chanteperdrix et al. 2002, Saurel and Abgrall 1999). This volume fraction is transported without any interface tracking. Low Mach number assumption applied to Euler equations leads to an hyperbolic system of conservation laws solved by appropriate fast numerical methods (Helluy et al. 2005).
More recently, some authors used a similar approach (Dias et al. 2010) and performed comparisons with the classical fully Navier-Stokes model (Braconnier et al. 2009). Our model should be considered as a compromise between computation cost and relevancy of physical modeling. Indeed, like in the Boussinesq approach, turbulence and viscosity are neglected which avoid to discretize the Laplacian operator and allow fast hyperbolic solver and therefore three dimensional computations. The equation of state of our average mixed model is artificial, but numerically relevant, and we do not need to build the interface like in VOF method (Kleeffsman et al. 2006). Such approach limits computation time and allow 3D simulations, which require up to now unusual computers for both SPH methods (e.g. Khayyer et al. 2009) and classical bi-fluid approach (see for example the work of Fuster et al. 2009 using the Gerris code with mesh refinement by octree).

The present study aims to analyse, by numerical modelling, the influence of macro- roughness on wave-breaking and run-up processes. By contrast to skin friction which only acts on the bottom shear stress, the presence of macro- roughness produces modifications of the flow field, i.e. accelerations and decelerations, up to the free surface. Our primary objective is thus to understand how the roughness elements will affect breaking dynamics, location of the breaking point, energy dissipation and run-up height. In this context, inviscid numerical model appears to be a relevant tool.

MATHEMATICAL MODEL

We use an eulerian two phases flow model leading to an hyperbolic system of conservation laws for mass and momentum. The convection of the air fraction satisfies a non-conservative equation. Moreover, an optimized artificial compressibility approach at low Mach number allows a fully explicit scheme.

We consider a 3D, compressible, inviscid two fluids flow model. The unknowns, the density $\rho(x, y, z, t)$, the three components of the velocity $\vec{u}(x, y, z, t)$, the pressure $p(x, y, ,z\ t)$ and the fraction of water $\varphi(x, y, z, t)$ depend on the spatial position (x, y, z) and the time t. The volume fraction satisfies $0 \leq \varphi \leq 1$, with herein $\varphi = 1$ in the water and $\varphi = 0$ in the air. Considering the gravity g, neglecting viscous effects and superficial tension, but introducing artificial compressible effects, we consider the following 3D Euler equations:

$$\frac{\partial W}{\partial t} + \nabla \cdot F(W) = S(W) \qquad \text{(1-a)}$$

$$\frac{\partial \varphi}{\partial t} + \vec{u}.\nabla \varphi = 0 \qquad \text{(1-b)}$$

In the isothermal model, the conservative variables vector W, the fluxes F and the source S are defined by

$$W = \begin{bmatrix} \rho \\ \rho u \\ \rho v \\ \rho w \end{bmatrix}, \quad F = \begin{bmatrix} \rho u & \rho v & \rho w \\ \rho u^2 + p & \rho uu & \rho wu \\ \rho uv & \rho v^2 + p & \rho wv \\ \rho uw & \rho vw & \rho w^2 + p \end{bmatrix} \text{ and } S = \begin{bmatrix} 0 \\ 0 \\ 0 \\ -\rho g \end{bmatrix}$$

$$p = p(\rho, \varphi)$$

In this model, the pressure depends on the volume fraction. In this way, it is possible to distinguish between the liquid and the gas. We have to provide an adequate Equation Of State (EOS). Let $c\ (x, y, z\ t)$ denotes the sound speed. It is usually admitted in physics that a flow is incompressible if the Mach number $M = \sqrt{u^2 + v^2 + w^2}/c$ is lower than $1/10$. Here, the real (physical) Mach number is generally much smaller, of the order of $1/400 \sim 1/1600$.

This is very constraining if an explicit finite volume solver is used because the time step Δt has to satisfy a CFL condition of the form

$$\Delta t \leq \alpha \frac{h}{\sqrt{u^2 + v^2 + w^2} + c} \qquad (2)$$

Where α is the CFL number, h the space step (for example the volume over the surface of the cell) and c the sound speed. Furthermore, it is known that numerical accuracy decreases due to the low Mach number of the flow. For those two reasons we have been led to choose an artificial pressure law where the sound speed is approximately fixed to $20\ m.s{-}1$. A very simple choice of EOS is the isothermal gas EOS that reads

$$p = c_0^2(\rho - (\varphi\, \rho_A + (\varphi - 1)\rho_W)) + p_0, \qquad (3)$$

Remark 1: This numerical model was previously based on a stiffened gas EOS, involving an energy conservation equation (Golay and Helluy, 2007). Numerical results showed that, in the case of a solitary wave breaking, the isothermal EOS is physically and numerically relevant. It allows a significant CPU time saving by avoiding penalizing CFL conditions due to fast pressure oscillations.

Remark 2: In our computations the flow velocity will typically be of the order of $1m/s$. An optimized value of artificial sound speed $c_0 = 20m/s$ has been chosen to limit, on one hand, the compressibility effects and, on the other hand, the numerical diffusion and the CFL constrain.

Remark 3: Our pressure law has no physical meaning inside the mixture zone $0 < \varphi < 1$ appearing due to numerical diffusion effects. More relevant models such in (Plumerault et al. 2009) could be investigated.

NUMERICAL METHOD

We use a finite volume approximation with an exact Riemann solver (Godunov's scheme). To avoid pressure oscillations of Godunov scheme occuring in multifluid cases, we use a method preserving moving contact discontinuity (Abgrall 1996). This condition leads to a non-conservative discretization (1-b). To use a fully conservative scheme, it would be necessary to consider a pressure law imposing pressure equilibrium of the two components (Chanteperdrix et al 2002, Allaire et al 2002).

In order to get the interface with accuracy, we use a second order approximation in time and space (MUSCL). The time discretization is explicit (midpoint Euler) and for the space discretization we use slope reconstruction. In two-fluid problems, it is often necessary to perform an additional slope limitation at the interface between the two fluids. For these reasons, the Barth limiter (Godlewski and Raviart 1996), which is faster and gives quite good results with competitive computing time in spite of a small distortion of the interface, has been selected. Details concerning the numerical methods can be found in (Golay and Helly 2007). Note that the effects of molecular and turbulent viscosities on the breaking process are here neglected. It allows a significant reduction in computation time. Moreover, as the breaking process is dominated the conversion from potential to kinetic energy and, in the presence of macro-roughness elements, by drag pressure forces, relevant analysis of the flow dynamics can be performed.

Remark 4: In order to capture accurately a sharp interface between air and water several numerical techniques, called "front sharpening" have been developed (e;g; Olsson et al. 2005). In our case, the method proposed by (Kokh et al. 2001), which add a sink term in the transport equation, appears to be an appropriate and simple method, and it will take place in further developments.

RESULTS

Computational configuration

In a first case, without influence of macro- roughness, we intend to break a wave over a reef. We consider on the right of $x = 5.225m$ a non-flat bottom equation $B(x, y) = (x - 5.225)/15$, in order to get the solitary wave breaking, the computational domain is $25\ m$ long and $2.5\ m$ high (Fig. 1). The precise boundary and initial conditions are depicted in figure 1. The initial condition is a stable solitary wave computed thanks to the method of Tanaka (1986): this is an incompressible potential solution of the Euler equations. The crest of the solitary wave is at $h = 0,6m$ over the still water level. It propagates at a phase velocity $v_p = 1.18\sqrt{gh} = 3.92m/s$. The Courant - Friedrichs - Levy number is fixed to 0.9. For the implementation, we have chosen a regular mesh made of hexahedra. The domain is approximated by a

coarse structured 3D finite volume grid: *3125* cells in the x-direction, *313* cells in the y-direction and one cell in the z-direction. A mirror condition is imposed on the lateral sides. A free boundary condition is imposed at the top and the height of the air layer is chosen in order to not significantly perturb the wave propagation.

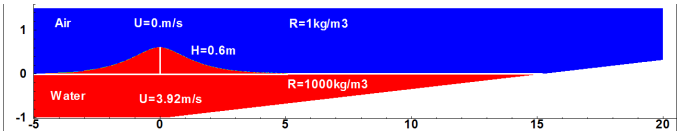

Fig.1: Wave breaking: solitary wave and reef

In order to avoid too long computations, we have also implemented a parallel version of the finite volume scheme, using the library message passing interface (MPI). The SGI parallel computer is made of 12 CPUs Itanium II at 1.5 GHz. The operating system is Linux RedHat. The domain is split into *N* sub-domains (*N=11* for the first case and 12 for the second). This solitary wave is propagated during 5s. The 2D simulations (about 1 million of cells) require 2 days CPU time.

Numerical results and analysis

Breaking wave over flat sloping bottom

First simulation case concerns the breaking of a solitary wave over a flat sloping bottom. Figure 2 present contours of fluid density at successive stages of the breaking process.

In a first stage [*0; 1.75s*] the wave propagates without deformation. Between *t=1.75* and *2.00s*, the wave progressively steepens and becomes more and more asymmetric during its propagation. After *t=2.00s*, the front face of the crest becomes nearly vertical and the breaking process starts, converting potential into kinetic energy. A fluid jet is ejected from the wave crest (Fig.2), and free falls under the action of gravity. The jet then impacts on the flat part of the free surface, inducing a characteristic overturning motion. The splash-up process develops when the jet rebounds on the free surface and probably partly pushes up the underlying water previously undisturbed (Lubin et al. 2006). The overturning motion then repeats two times, each successive cycle of jet ejection/impact/splash-up being weaker than the previous one. Gas pockets are trapped into the vortices cores and do not diffuse too much during the simulation time.

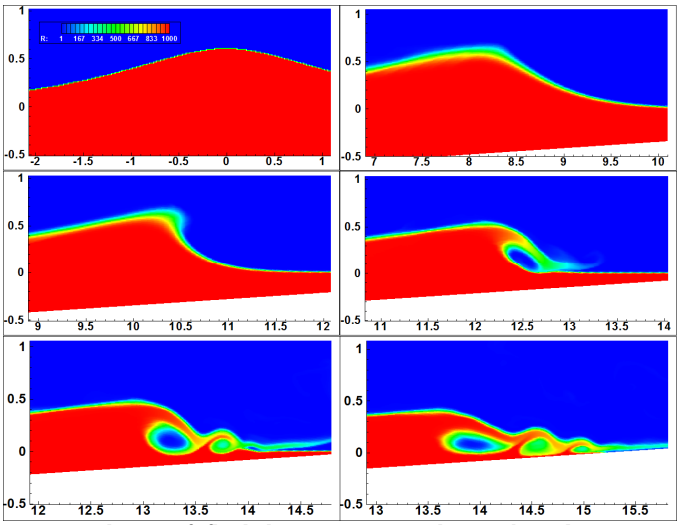
Fig.2. Evolution of fluid density contours during the solitary wave breaking on a flat sloping bottom at times *t=0s; 2.0s; 2.5s; 3.s; 3.25s; 3.5s* (kg.m^{-3}).

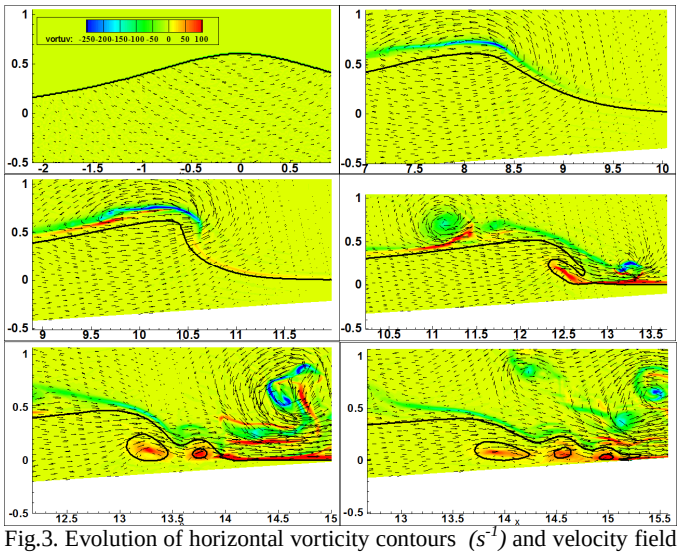
Fig.3. Evolution of horizontal vorticity contours *(s^{-1})* and velocity field during the solitary wave breaking on a flat sloping bottom at times *t=0s; 2.0s; 2.5s; 3.s; 3.25s; 3.5s.* Free surface is shown by isoline *φ= 0.5*.

Figure 3 shows contours of vorticity during the solitary wave breaking for the flat sloping case and for different times of simulation. During the wave propagation [*0; 2.5s*], a thin sheared layer of negative vorticity is observed on the free surface. As the crest steepens (*t=2.5s*), the negative vorticity layer thickens and the vorticity magnitude strongly increase on the top of the wave where the jet starts to form. Thin layer of negative vorticity is observed above the free surface in the front of the wave, indicating the initiation of the overturning motion. Another thin negative vorticity layer develops behind the crest just above the free surface, probably related to the air acceleration motion as showed by Lubin et al. (2006).

When the jet impacts the underlying free surface, one notes the formation of several strongly sheared zones, which reveals the overall vortical nature of the breaking process. First, the air trapped under the falling jet tends to flow out which induces the intense positive vorticity layer on the water surface. The ejected air then recirculates behind the falling water jet until the complete connection of water masses.

The wake of the crest is also strongly rotational, showing several patches of negative and positive vorticity. The crest wake then organizes (*t=3.5s*) with the formation of a large coherent vortex structure of negative sign, i.e. with an anti-clockwise fluid motion. Near the bottom, the successive splash-up processes are clearly shown by three positive vorticity zones. This corresponds to the co-rotative motion into the three air pockets observed on figure 2, as noted by Miller (1976) or Sakaï et al. (1986).

Figure 4 presents the evolution of water surface profile during the wave propagation and breaking. This confirms the features exposed above: the progressive steepening of the wave, the jet ejection from the crest and rebound on the previously undisturbed free surface, and the three successive splash-up cycles.

Overall features are in good agreement with wave breaking results presented in literature (e.g. Christensen 2006, Lubin et al. 2006).

Considering these simulations as a validation step, our numerical model gives satisfactory and encouraging results for this 2D configuration. Nevertheless, quantitative comparisons with experimental data will still be investigated.

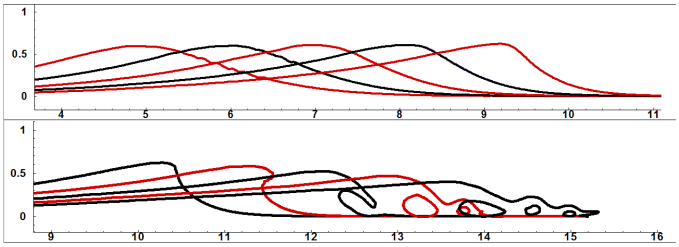

Fig.4. Free surface profiles (isoline $\varphi=0.5$) during wave propagation and breaking (*1.25s; 1.5s; 1.75s; ;2.25s; 2.5s; 2.75s; 3.s; 3.25s; 3.5s*) .

Breaking wave over macro-roughness elements

In this section, we present results we obtain at the simulation of wave-breaking and run-up processes over sloping bottom covered by rectangular macro-roughness elements. This case will be referred hereinafter as the "rough" case. The initial conditions and configurations are the same as the previous case except for the bottom (fig.5). The macro-roughness elements are *0.2 m* wide and *0.2 m* high and are distant from *0.4m.*

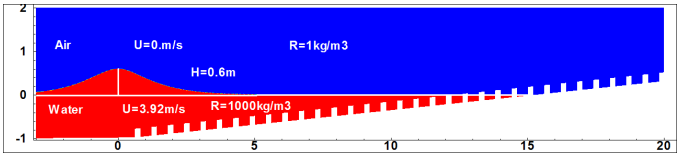

Fig.5: Wave breaking: solitary wave and reef with macro-roughness

Figure 6 present contours of fluid density at successive stages of the breaking process over a non flat sloping bottom. Analogical results are noticed apart from the fact that the breaking process starts earlier comparing to the case without macro-roughness. The overturning motion then repeats two times, each successive cycle of jet ejection/impact/splash-up being weaker than the previous one.

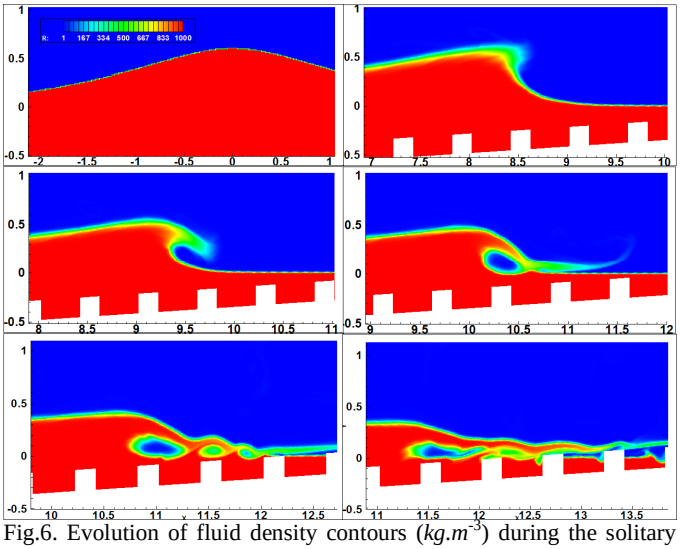

Fig.6. Evolution of fluid density contours ($kg.m^{-3}$) during the solitary wave breaking on a rough sloping bottom at times *t=0s; 2.0s; 2.25s; 2.5s; 2.75s; 3.00s.*

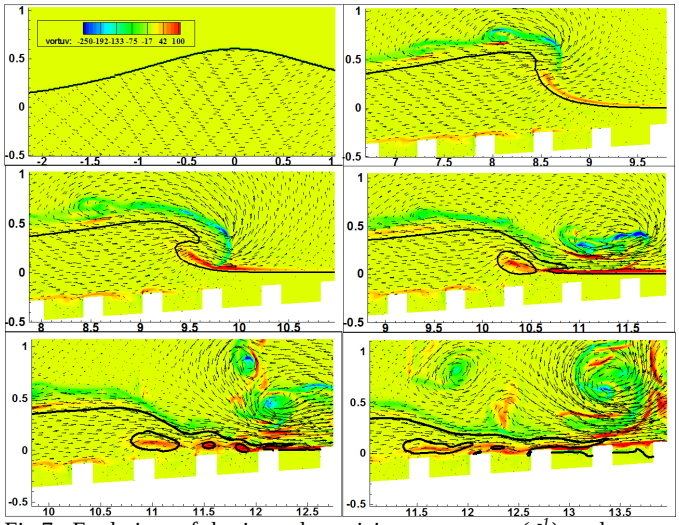

Fig.7. Evolution of horizontal vorticity contours (s^{-1}) and vector velocity field during the solitary wave breaking on a rough sloping bottom at times *t=0s; 2.0s; 2.25s; 2.5s; 2.75s; 3.00s.* Free surface is shown by isoline $\varphi= 0.5$.

Figure 7 shows contours of vorticity during the solitary wave breaking for the non-flat sloping case and for different times of simulation. We note that the vorticity generated in this case of is much more important than previously but the surge mechanism is the same.

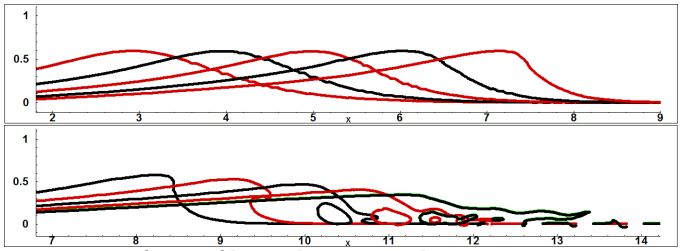

Fig.8. Free surface profiles (isoline $\varphi= 0.5$) during wave propagation and breaking (*0.75s; 1.0s*; *1.25s; 1.5s; 1.75s; 2.25s; 2.5s; 2.75s; 3.0s*) .

Figure 8 presents the evolution of water surface profile during the wave propagation and breaking. The progressive steepening of the wave, the jet ejection from the crest and rebound on the previously undisturbed free surface, and the successive splash-up cycles.
It should be noted that, as we consider an isolated wave breaking event, the complex hydrodynamics induced by the breaking of regular incoming waves can not be represented, and thus the interactions between waves and wave-induced currents can not be analysed from the present numerical simulation. It can however be expected that the bottom return flow should be strongly influenced by the presence of macro-roughness.

Comparison between rough and flat bottom case

In this section, we analyse, by numerical modelling, the influence of macro-roughness on wave-breaking, how the presence of macro-roughness produces modifications of the flow field and how the roughness elements will affect breaking dynamics, location of the breaking point.

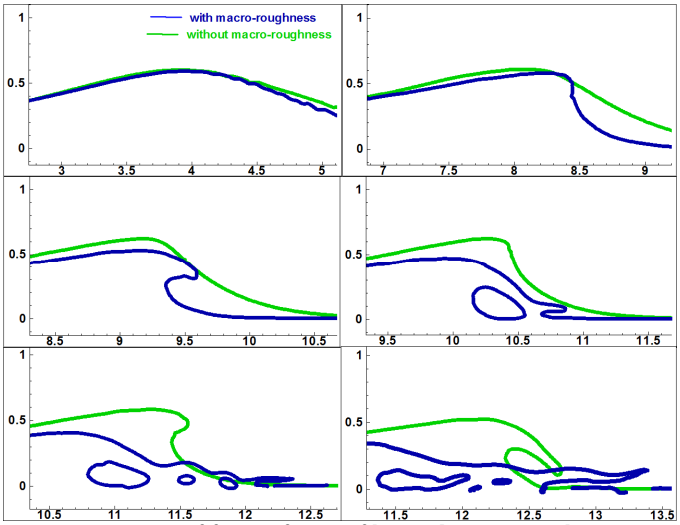

Fig.9. Comparison of free surface profiles (isoline $\varphi = 0.5$) during wave propagation and breaking *(1.0s;2.00s; 2.25s; 2.50s; 2.75s; 3.0s*) between rough (blue) and flat bottom case (green)

Comparison between flat and rough case is shown on figure 9 at different time of simulation for free surface profiles. We immediately noticed the strong influence of the rough bottom that causes the slowdown of the wave, a change in the morphology of the surge and the progress of the breaking point. The spread and swelling of the incident wave are quickly affected by the presence of macro-roughness. One explanation for this is that the wave in the rough boundary case breaks slightly earlier (Fig.11), and thereby a considerable amount of energy is lost during the breaking process.

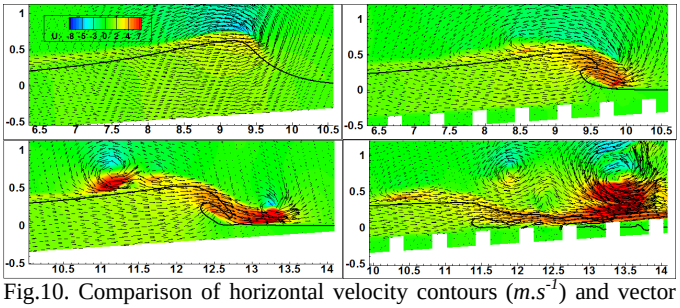
Fig.10. Comparison of horizontal velocity contours ($m.s^{-1}$) and vector velocity field at *t=2.25s and t=3.00s* between rough (left) and flat bottom case (right).

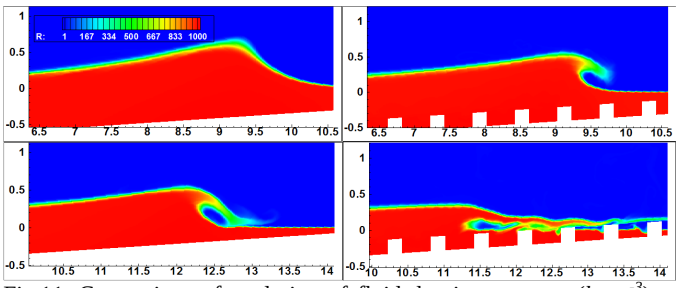
Fig.11. Comparison of evolution of fluid density contours ($kg.m^{-3}$) at *t=2.25s and t=3.00s* between rough (left) and flat bottom case (right)

Figures 10 and 11 present comparisons between rough and flat bottom cases at *t=2.25s* and *t=3.00s* for horizontal velocity fields and fluid density contours, respectively.
It clearly indicates that the wave crest is strongly accelerated by the presence of macro-roughness elements over the bottom. Indeed, as a momentum deficit layer develops around the roughness elements due to the form drag, a momentum excess necessarily focuses in the upper part of the wave. The increase of horizontal velocity thus induces the earlier breaking for the rough case, as shown on figure 10. We observe that the surge form associated with the presence of macro-roughness causes the development of a layer of near-zero speed.

Comparison between the two rough cases

In this section we compare computational results we obtain with two rough cases. The first case (rough case 1) is the one studied before and for the second the macro-roughness elements are *0.2 m* wide and *0.2 m* high and are distant from *0.8m (0.4m* for the first one*).*

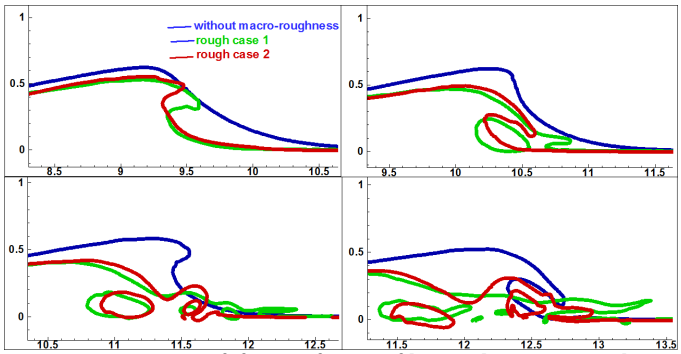

Fig.12. Comparison of free surface profiles (isoline $\varphi = 0.5$) during wave propagation and breaking at $t = 2.25s$ and $t = 2.50ss$ between rough case 1 (green), rough case 2 (red) and flat bottom case (blue).

The breaking process starts earlier for the first case and one notes a positive vorticity layer just above the macro-roughness for two cases (Fig.13). The recirculation of water is more developed in the second case, this was not highlighted in the other one witch the distance of macro-roughness is too small. It has roughly equivalent to a condition of zero speed limits at the wall **.**

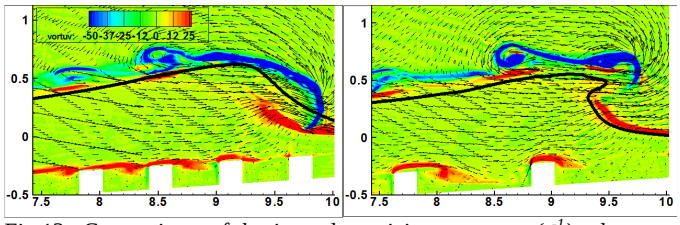
Fig.13. Comparison of horizontal vorticity contours (s^{-1})and vector velocity field during the solitary wave breaking between rough case 1 (left), rough case 2 (right) $t = 2.25s$. Free surface is shown by isoline $\varphi = 0.5$.

The observed qualitative features, such as the slowing down of the solitary wave propagation and the downslope motion of the breaking point have obviously been confirmed.
The implementation of artificial compression technique (e.g. Olsson and Kreiss 2005) or local mesh refinement method (e.g. Jing-Song et al. 2007) are now under consideration to improve the interface description.

CONCLUSION

In this paper, numerical simulations of solitary wave breaking are performed solving Euler equations for a two phases flow model based

on a hyperbolic system of conservation laws. The physical aim of the study is to understand the influence of macro-roughness elements on the wave breaking dynamics.

The numerical model gives satisfactory results for the breaking on a sloping bottom with and without roughness elements. The numerical tool accurately reproduced the overturning motion, the entrainment of air pockets, the splash-up occurrence, the dynamics generated by plunging breaking waves and the generation of coherent vortex structures highlighted in the literature.

In presence of roughness elements on the sloping bottom, the increase of horizontal velocity has a major influence on the wave propagation and breaking and accelerates the reversal of the wave.

Interface compression and mesh refinement methods are now under consideration to improve the interface description.

A parametric study of the geometry and density of the macro-roughness is necessary before proposing a comprehensive analysis of physical processes involved in the surge of funds rough.

ACKNOWLEDGEMENTS

Prof. P. Helluy is warmly acknowledged for his help in the numerical code development and assessment. This work was granted by TSUMOD project french Agence Nationale de la Recherche ANR-05-CATT-O16. Computations were performed on the Regional PACA – Conseil Général 83 SOCOM cluster.

REFERENCES

Abgrall, R, (1996). “How to prevent pressure oscillations in multicomponent flow calculations: a quasi-conservative approach”, *J Comput Phys*, Vol 125, No 1, pp 150–160.

Allaire, G, Clerc, S and Kokh, S, (2002). "A five-equation model for the simulation of interfaces between compressible fluids", *J Comput Phys*, Vol 181, pp 577-616.

Barberon, T, Helluy, P and Rouy, S, (2003). "Practical computation of axisymmetrical multifluid flows", *International Journal of Finite Volumes*, Vol 1, No 1, pp 1–34.

Biausser, B, Guignard, S, Marcer, R and Fraunié, P, (2004). "3D two phase flows numerical simulations by SL-VOF method", *Int J Num Meth in Fluids*, Vol 45, No 6, pp 581-604.

Braconnier, B, Hu, JJ, Niu, YY, Nkonga, B and Shyue, KM, (2009). "Numerical simulation of low Mach compressible two-phase flows: preliminary assessment of some basic solution techniques", *ESAIM: Proceeding*, August 2009, Vol. 28, pp 117-134

Chanteperdrix, G, Villedieu, P and Vila, J-P, (2002). "A compressible model for separated two-phase flows computations", *ASME Fluids Engineering Division Summer Meeting*, July 2002 (ASME: Montreal, Canada).

Christensen, E D, (2006). "Large eddy simulation of spilling and plunging breakers", *Coastal Engineering*, Vol 53, pp 463-485.

Dias, F, Dutykh, D and Ghidaglia, J M, (2010). "A two-fluid model for violent aerated flows", *Computers & Fluids*, Vol 39, No 2, pp 283-293.

Fuster, D, Agbaglah, G, Josserand, C, Popinet, S and Zaleski, S, (2009). "Numerical simulation of droplets, bubbles and waves: state of the art", *Fluid Dyn Res*, Vol 41, No 6.

Gallouet, T, Hérard, JP and Seguin, N, (2003). " Some approximate Godunov schemes to compute shallow-water equations with topography", *Computers and Fluids*, Vol 32, No 4, pp 479–513.

Godlewski, E and Raviart, P-A, (1996). "Numerical approximation of hyperbolic systems of conservation laws", *Applied Mathematical Sciences*, Vol 118, Springer-Verlag, New York.

Golay, F and Helluy, P (2007). "Numerical schemes for low Mach wave breaking", *International Journal of Computational Fluid Dynamics*, Vol 21, No 2, pp 69–86.

Grilli, S T, Skourup, J and Svendsen, I A, (1989). "An efficient boundary element method for nonlinear water waves", *Engineering Analysis with Boundary Elements*, Vol 6, No 2, pp 97–107.

Grilli, S, Guyenne, P and Dias, F, (2001). "A fully non-linear model for three-dimensionnal overturning waves over an arbitrary bottom", *Int J Numer Meth Fluids*, Vol 35, pp 829-867.

Guignard, S, Marcer, R, Rey, V, Kharif, C and Fraunié, P, (2001). "Solitary wave breaking on sloping beaches: 2-D two phase flow numerical simulation by SL-VOF method", *Eur J Mech B Fluids*, Vol 20, No 1, pp 57-74.

Guyenne, P and Grilli, S T, (2006), "Numerical study of three-dimensional overturning waves in shallow water", *J Fluid Mech*, Vol 547, pp 361–388.

Helluy, P, Golay, F, Caltagirone, J P, Lubin, P, Vincent, S, Drevrard, D, Marcer, R, Fraunié, P, Seguin, N, Grilli, S, Lesage, A N, Dervieux, A and Allain, O (2005). "Numerical simulation of wave breaking", *M2AN*, Vol 39 no 3, pp 591-607.

Jing-Song, B, Ping, L, Li-Yong, Z and Tao, W, (2007). "A quadtree adaptive level set method for capturing interfacial instability on Cartesian grid", *Engineering Applications of Computational Fluid Mechanics* Vol 1, No 4, pp.263-272.

Khayyer , A, Gotoh, H and Shao, S, (2009). "Enhanced predictions of wave impact pressure by improved incompressible SPH methods", *Applied Ocean Research*, Vol 31, No 2, pp 111-131.

Kleefsman, K M T, Fekken, G, Veldman, A E P, Iwanowski, B and Buchner, B, (2005). "A Volume-of-Fluid based simulation method for wave impact problems", *J Comput Phys*, Vol 206, pp 363–393.

Kokh, S, (2001). "Aspects numériques et théoriques de la modélisation des écoulements diphasiques compressibles par des méthodes de capture d'interfaces", *Phd Thesis*, Université Paris 6 (in French).

Lubin, P, Vincent, S, Abadie, S and Caltagirone, J P, (2006) “Three-dimensional Large Eddy Simulation of air entrainment under plunging breaking waves”, *Coastal Eng*, Vol 53, pp 631-655.

Miller, R L, (1976). “Role of vortices in surf zone prediction: sedimentation and wave forces”, *Soc. Econ. Paleontol. Mineral. Spec Publ*, Vol 24, Ed. R. A. Davis, R. L. Ethington, pp 92-114.

Olsson, E and Kreis,s G, (2005). “A conservative level set method for two-phase flow”, *J Comput Phys*, Vol 210, pp 225-246.

Peregrine, D H, (1983). “Breaking waves on beaches”, *Annu Rev FIuid Mech*, Vol 15, pp 149- 78

Plumerault, R, Astruc, D, Mory, M, Maron, P and Villedieu, P, (2009). "Simulations de l'impact de vagues sur une structure verticale prenant en compte la compressibilité du liquide", *proceeding du congrès français de mécanique*, Marseille, Août 2009 (in French).

Sakaï, T., T. Mizutani, H. Tanaka and Y. Tada. (1986). “Vortex formation in plunging breaker”, *Proceedings of 20th International Conference on Coastal Engineering*, ASCE, 711-723.

Saurel, R and Abgrall, R, (1999). "A simple method for compressible multifluid flows", *SIAM J Sci Comput*, Vol 21, No 3, pp 1115–1145.

Tanaka, M, (1986). "The stability of solitary waves", *Phys Fluids*, Vol 29, No 3, pp 650-655.

Vincent, S, Caltagirone, J P, Lubin, P and Randrianarivelo, T, (2004). "An adaptive augmented Lagrangian method for three-dimensional multimaterial flows", *Computers and Fluids*, Vol 33, No 10, pp 1273-1289.

Yasuda, T, Mutsuda, H and Mizutani, N, (1997). "Kinematic of overturning solitary waves and their relations to breaker types", *Coastal Engineering*, Vol 29, pp 317–346